Effects of Processing Parameters on the Grain Refinement of Magnesium Alloy by Equal-Channel Angular Extrusion

S.X. DING, C.P. CHANG, and P.W. KAO

The Mg-3 pct Al-1 pct Zn (AZ31) alloy has been used as a model material for understanding the grain-refinement process of a Mg alloy fabricated by equal-channel angular extrusion (ECAE). The effects of ECAE processing parameters on grain refinement have also been studied; it was found that these effects are quite different from those for fcc metals. A multitemperature extrusion procedure has been developed, which can produce an ultrafine-grained AZ31 alloy having a grain size 0.37 μm. For the AZ31 alloy, this ultrafine-grained alloy has a record high strength accompanied by reasonably good tensile ductility. The success of the development of this ECAE procedure proves that ECAE can offer a good opportunity for the development of high-strength Mg alloys.

DOI: 10.1007/s11661-008-9747-3

I. INTRODUCTION

THE ability to produce bulk ultrafine-grained metals by equal-channel angular extrusion (ECAE), also called equal-channel angular pressing, has garnered a tremendous amount of attention over the last decade. The literature reflects the many attempts that have been made to investigate the factors responsible for the grain-refinement process in ECAE.

The amount of plastic strain that is imposed on a billet is an important processing parameter for the production of ultrafine-grained metals. For fcc and bcc metals, by continuously imposing plastic strain, grains are gradually refined. The refinement process is achieved through the continuous subdivision of the original grains by dislocation walls, *e.g.*, References 1 through 3. This process proceeds homogeneously over the entire billet. For aluminum, as the imposed plastic strain is increased, dislocation walls gradually transform into grain boundaries; meanwhile, misorientations across the boundaries are increased.[4] For copper, due to its low stacking-fault energy, the transformation of dislocation walls into grain boundaries is difficult,[5–7] but misorientations across the boundaries still increase with increasing strain.

Apart from the imposed plastic strain, the channel angle, Φ, is another important processing parameter that can influence the grain-refinement process. The first and most systematic study of the influence of the die angle on grain refinement was published by Nakashima *et al.*[8] Their results suggested that the smaller the die angle, the more effective the grain-refinement process.

The process route has also been reported to have a significant effect on the grain-refinement process.[2,9,10] Through detailed analysis of the extruded microstructure of aluminum by transmission electron microscopy (TEM), Sun *et al.*[9] reported that route B_c is the most effective route in terms of grain refinement.

Extrusion at elevated temperatures can prevent the cracking of hard materials and thus improve the workability of a billet.[11] When the extrusion temperature was increased, the minimum attainable grain size was found to be increased and the fraction of high misorientation boundaries was found to be lower.[12–14]

The workability of a billet was reported to be improved significantly by using a low extrusion speed to process titanium and 4340 steel.[11] The extrusion speed was reported[15] to have no influence on the grain size of aluminum and its alloys subjected to ECAE.

Despite the fact that the aforementioned conclusions were mainly drawn from the experimental results involving fcc metals, they appeared to be widely accepted in the literature regardless of the crystal structure of the material being processed.

Over the last few years, magnesium alloys have become promising candidates for the replacement of some conventional engineering metals because of the demand of lighter structural materials. The ECAE process has been used to refine the grain size of magnesium alloys, in order to improve their mechanical properties.

Many authors (*e.g.*, in References 16 through 30) have reported that by using ECAE at elevated temperatures, the grain size of magnesium alloys can be dramatically reduced. In the case of the AZ31 alloy,[20–30] the reported grain size after ECAE ranged from 6 to 0.7 μm, due to the different processing parameters used. Because there is no systematic study of the effect of ECAE processing parameters on the grain-refinement process of magnesium alloys, these conclusions about the effects of the processing parameters on grain refinement, which were drawn from fcc metals, were widely adopted for the discussion in the literature of the processing of magnesium alloys. For example, Mukai *et al.*[20] mentioned that the reason that route B_c was used to process their Mg

S.X. DING, Research Student, and C.P. CHANG and P.W. KAO, Professors, are with the Institute of Materials Science and Engineering, National Sun Yat-sen University, Kaohsiung, 80424 Taiwan, Republic of China. Contact e-mail: cpchang@mail.nsysu.edu.tw
Manuscript submitted May 8, 2008.
Article published online January 6, 2009

alloy was due to the result given by Iwahashi *et al.*,[10] in which route B_c was reported to be more effective in producing high-angle boundaries in aluminum. Perhaps this is the reason why virtually all researchers used route B_c to process their Mg alloys,[16–29] despite the fact that there is no report showing that route B_c is the best process route for refining the grain size of Mg alloys. Many authors[20,21,24–27,29] used a large number of extrusion passes, *e.g.*, 6 or 8 passes, to process their Mg alloys; this was also based on the results for fcc metals, for which a large plastic strain was required to obtain a fine-grained structure. However, Jin *et al.*[29] reported that the grain size remained unchanged after only 4 extrusion passes; this raises the question about the plastic strain required to achieve a fine-grained structure in Mg alloys, specifically, whether the plastic strain will be similar to that for fcc metals.

It might be thought that, if the grain-refinement process for two materials is the same, the effect of the processing parameters on the grain refinement should also be the same. The grain-refinement process of fcc metals, as mentioned earlier, is reasonably clear thus far; however, for Mg alloys, with their hexagonal crystal structure, the process is not yet clear. Kim and Kim[23] found a bimodal distribution of grain size after 1 extrusion pass; because the existence of equiaxed grains was discovered after the passes that followed, they suggested that dynamic recrystallization occurred during ECAE. However, they believed that the generation of new grains was due not to a process of nucleation and growth, but to the gradual transformation of low-angle subgrain boundaries into high-angle grain boundaries through the absorption of dislocations generated during ECAE, as was proposed for aluminum.[4] Xia *et al.*[26] also found a heterogeneous grained structure after the first few extrusion passes. They suggested that the refinement process was due to the fact that some grains, having favorable orientations and having been deformed first, were also refined first. As the number of extrusion passes increased, deformation spread into the other grains; subsequently, fine grains formed in the whole structure and the grain-refinement process was completed. Jin *et al.*[29] also suggested that the process of grain refinement consisted of the gradual transformation of low-angle subgrain boundaries into high-angle grain boundaries due to continuous dynamic recovery and recrystallization. Su *et al.*[28] adopted a different view: They suggested that, after the original grains were deformed, dynamic recovery and the nucleation of new grains occurred. They also suggested that the continuous heating of the billet in the die during extrusion caused the static growth of both the recovered subgrain boundaries and the newly formed recrystallized grains; eventually, they believed, homogeneously distributed fine grains occupied the whole billet. The problem with this mechanism is that it cannot explain the formation of the heterogeneous distribution of bimodal grains in the early stage of the grain-refinement process, which was reported by many authors, *e.g.*, References 21 through 23, and 25, 26, and 29.

From the point of view of the present authors, the results reported in the literature indicate that the grain-refinement process of Mg alloys appears to be different from that of fcc metals. Therefore, the ECAE processing parameters that govern the grain refinement of Mg alloys need to be examined; this is the aim of the present research. It is also interesting to know to what extent the grain size of Mg alloys can be refined by optimizing the ECAE processing parameters. The AZ31 Mg alloy has been chosen as the model material for the present research, because it is an important wrought-Mg alloy and it has a simple microstructure, *i.e.*, a single-phase solid-solution alloy.

II. EXPERIMENTAL

Hotrolled 1.25-cm-thick AZ31 (Mg-3 pct Al-1 pct Zn) plate from Magnesium Elektron (Manchester, UK) was used in the present research. Its nominal composition is 3.0 wt pct Al, 1.0 wt pct Zn, 0.2 wt pct Mn, and balanced magnesium. There is a strong basal fiber texture (*c* axes of the hcp structure) that is primarily aligned parallel to the normal direction of the plate. The material was annealed at 345 °C for 12 hours; it was then air cooled to room temperature. The grain size of the homogenized material is 7 μm. The equivalent circle diameter is used to represent the grain size throughout this article. Billets $1.2 \times 1.2 \times 10$ cm in size were cut from the plate, with their long sides parallel to the rolling direction of the plate. Two ECAE dies, with die angles of $\Phi = 90$ and 120 deg, were used. The outer die angle (Ψ), defining the outer arc of two channels, is 0 deg for both dies. The equivalent strains imposed on a billet by the die having $\Phi = 120$ and 90 deg are 0.67 and 1.15, respectively. Heating jackets were put on both dies, and the extrusion temperature was controlled within ±5 °C of the setting temperature. During extrusion, the billet was inserted into the entrance channel of the heated die and stayed in the channel for approximately 3 minutes, to allow the billet to reach the targeting temperature. After extrusion, the billet was quenched into water. Three axes, *x*, *y*, and *z*, were used to define the coordinate system of the channels and the specimen after extrusion, as shown in Figure 1. Unless specified, all billets were extruded by putting the rolling plane of the plate parallel to the *xz* plane of the entrance channel. Conventionally defined routes A, B_c, and C[31] are used in this article.

After extrusion, specimens for grain size measurement were cut parallel to the *xz* plane of the billets. After mechanical polishing, specimens were etched for 2 to 3 seconds using a solution of 10 mL acetic acid, 4.2 g picric acid, 10 mL water, and 70 mL ethanol and then quickly transferred into an ethanol bath, to minimize the oxidation of the specimens. A JEOL* 6330 field-emission scanning electron microscope (SEM) was used to examine the specimens. The operation voltage for the secondary electron image was 5 kV. A low acceleration voltage was used due to the poor conductivity of the

*JEOL is a trademark of Japan Electron Optics Ltd., Tokyo.

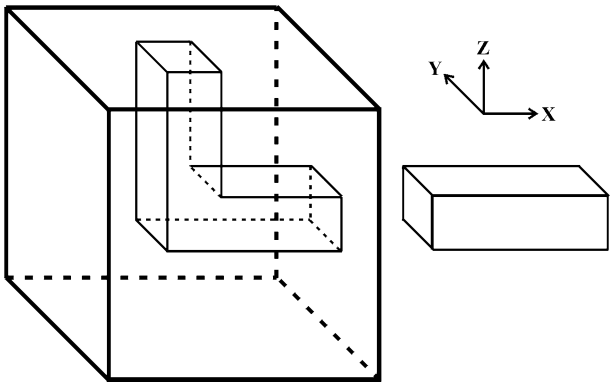

Fig. 1—The geometry and coordinate axes of the ECAE die and the billet.

surface reaction layer of the specimens after etching. The standard operation voltage, *e.g.*, 20 kV, often causes a charging effect to a certain degree and results in a poor image. Grain boundaries were manually marked on the micrographs; additionally, through the use of the Optimas computer program (BioScan Inc., Washington), the equivalent circle diameter and the aspect ratio of every grain were determined. The aspect ratio is defined as the ratio of the major and minor axes of an ellipse that best fits the shape of the grain. For each specimen, SEM images of six randomly selected areas obtained from near the central part of the specimen were taken. The total number of grains analyzed was approximately 7000 for each specimen. An HKL CHANNEL (Oxford Instrument, Oxfordshire, UK) 5 system attached to the JEOL 6330 field-emission SEM was used for the analysis of the boundary misorientations through electron backscatter diffraction (EBSD). The specimens for EBSD analysis were prepared by conventional mechanical grinding, followed by a mechanical polishing with a diamond paste and a final polishing with colloidal silica. For EBSD orientation mapping, the scanning step was 0.1 μm and the dwell time for each pattern was 240 ms. The thin foils for TEM were polished by a solution of 22.3 g magnesium perchlorate + 10.6 g lithium chloride + 200 mL 2-butoxyethanol + 1000 mL methanol, at −45 °C and 88 V; these were examined in a Philips** CM200 microscope.

**PHILIPS is a trademark of Philips Electronic Instruments Corp., Mahwah, NJ.

The mechanical properties of the specimens machined from the billets were evaluated. Tensile tests were carried out on an Instron 5582† universal testing machine with a constant strain rate of 3×10^{-3}/s. The dimension of the gage section of the tensile specimen was 4 × 1.5 × 16 mm. The stress direction was along the extrusion direction of the billet.

†Instron is the trademark of Instron Ltd., Buckinghamshire, UK.

III. RESULTS

To understand the grain-refinement process and the effect of the processing parameters on the grain refinement, the processing parameters have been systematically varied. The results are discussed in this section.

A. *Number of Extrusion Passes (Imposed Plastic Strain)*

To investigate the effect of the number of extrusion passes used, billets were extruded by the 120-deg die at 200 °C using route A; the extrusion speed was 10 cm/min. When the billets were examined after different extrusion passes, it was found that newly formed fine grains were observed immediately after the first pass, as shown in Figure 2. Figure 2(b) shows the coexistence of both fine and coarse grains. When the coarse grains were examined more closely, it was found that many grain boundaries were serrated. Many fine grains were formed along the grain boundaries of those coarse grains, which is a nucleation process typical for dynamic recrystallization. This type of partially dynamically recrystallized structure can be seen more clearly in the specimens extruded at 175 °C, as shown in Figure 3. When the number of extrusion passes was increased, the area covered by fine grains increased, while the width of the coarse grains became narrower (Figure 2(c)); eventually, the coarse-grained structure disappeared and a fine-grained structure resulted (Figure 2(d)). Figure 4 shows how the average grain size of the billet quickly reduced to a final-equilibrium fine-grained size, in this case, from 7 to approximately 2 μm. Despite the measured average grain size remaining virtually unchanged after the second extrusion pass, a few elongated coarse grains could still be found after the third extrusion pass. After 4 passes, the billet was completely transformed from a coarse-grained structure into a homogeneous fine-grained structure. Further extrusion could not effectively refine the grain size. Figure 5 shows the grain size distribution histogram obtained from an area of approximately 35,000 μm^2 for the specimen unextruded (Figure 5(a)), after 1 extrusion pass (Figure 5(b)), and after 4 extrusion passes (Figure 5(c)). Figure 5 indicates that grain size distribution showed little change after the first and fourth extrusion passes. The averaged grain aspect ratio of the billet before ECAE was 1.5. The averaged aspect ratio of dynamically recrystallized fine grains (grains smaller than 4 μm) after the first through the fourth extrusion passes is 1.8, 1.7, 1.7, and 1.7, respectively. These results show that both the size and the shape of these fine grains remained the same, irrespective of the number of extrusion passes used.

When EBSD was used to characterize the misorientations of the generated boundaries, it was found that most of the fine grains generated had high misorientation boundaries and that low-angle boundaries were formed within the coarse grains (Figure 6). Because etching could not reveal those low-angle boundaries formed within the original coarse grains, these boundaries cannot be seen in Figure 2. The TEM observations showed that most fine grains were in an equiaxed shape with clear grain-boundary fringes; the boundaries often

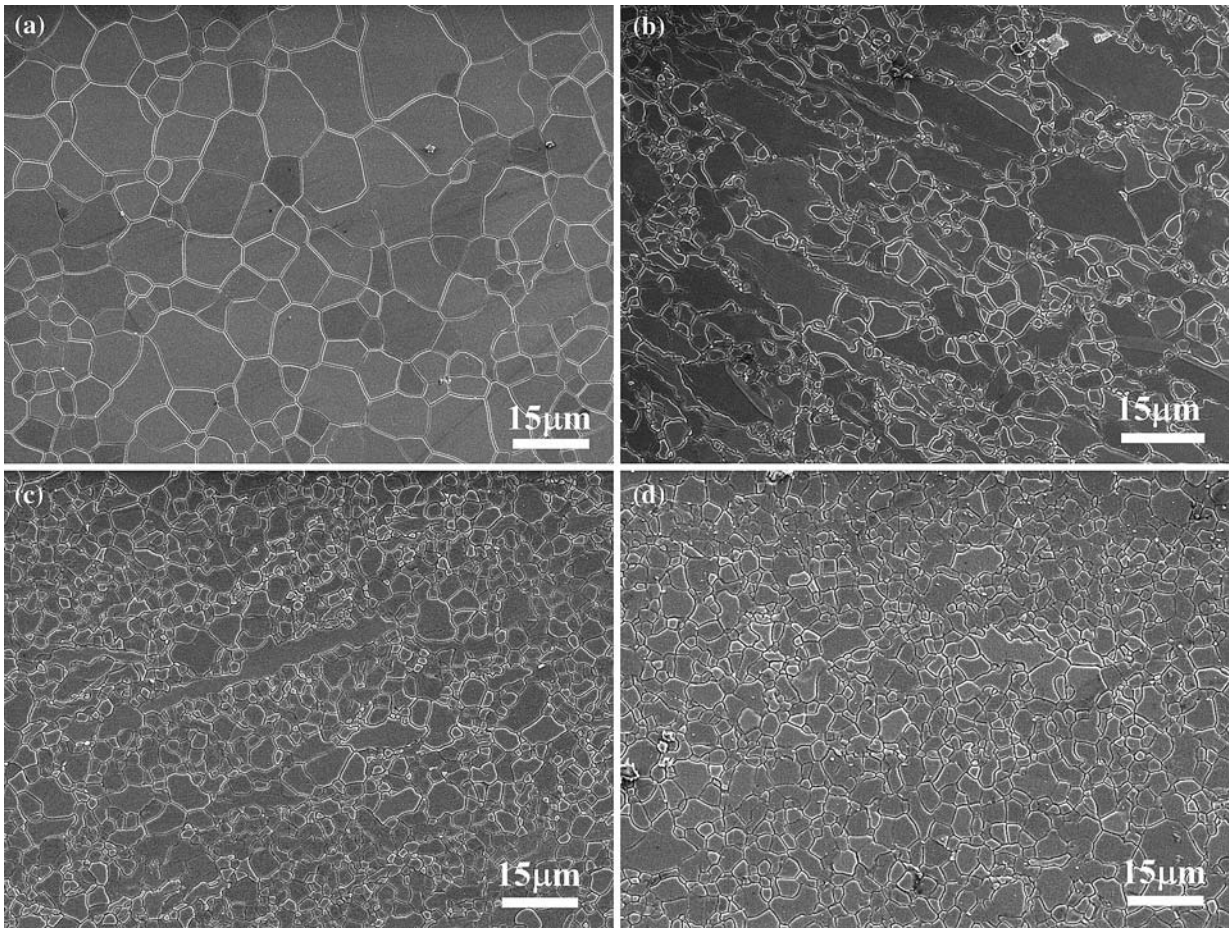

Fig. 2—SEM micrographs showing the microstructure of a billet extruded after (*a*) 0, (*b*) 1, (*c*), 2, and (*d*) 4 passes by Φ = 120-deg die, using route A at 200 °C; extrusion speed was 10 cm/min.

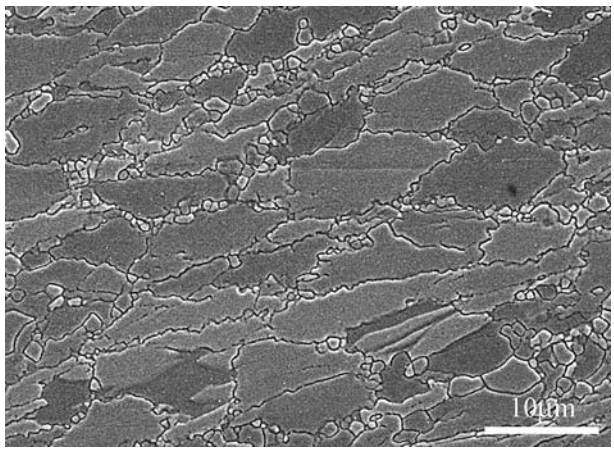

Fig. 3—SEM micrograph showing the microstructure of a billet after 1 extrusion pass by Φ = 120-deg die, using route A at 175 °C; extrusion speed was 10 cm/min. Note serration of original grain boundaries and nucleation of fine grains at original grain boundaries.

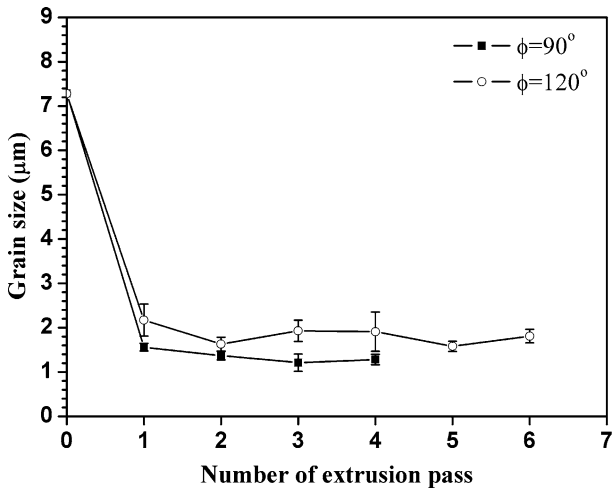

Fig. 4—Evolution of grain size as a function of an extrusion pass by two dies with different die angles. Route A was used, at 200 °C; extrusion speed was 10 cm/min.

met at a configuration of approximately 120 deg, indicating that these boundaries are equilibrium grain boundaries having a similar boundary energy. Figure 7 shows some fine grains formed alongside a coarse grain. The grain-boundary fringes and the equilibrium-boundary configuration associated with these fine grains should be noted.

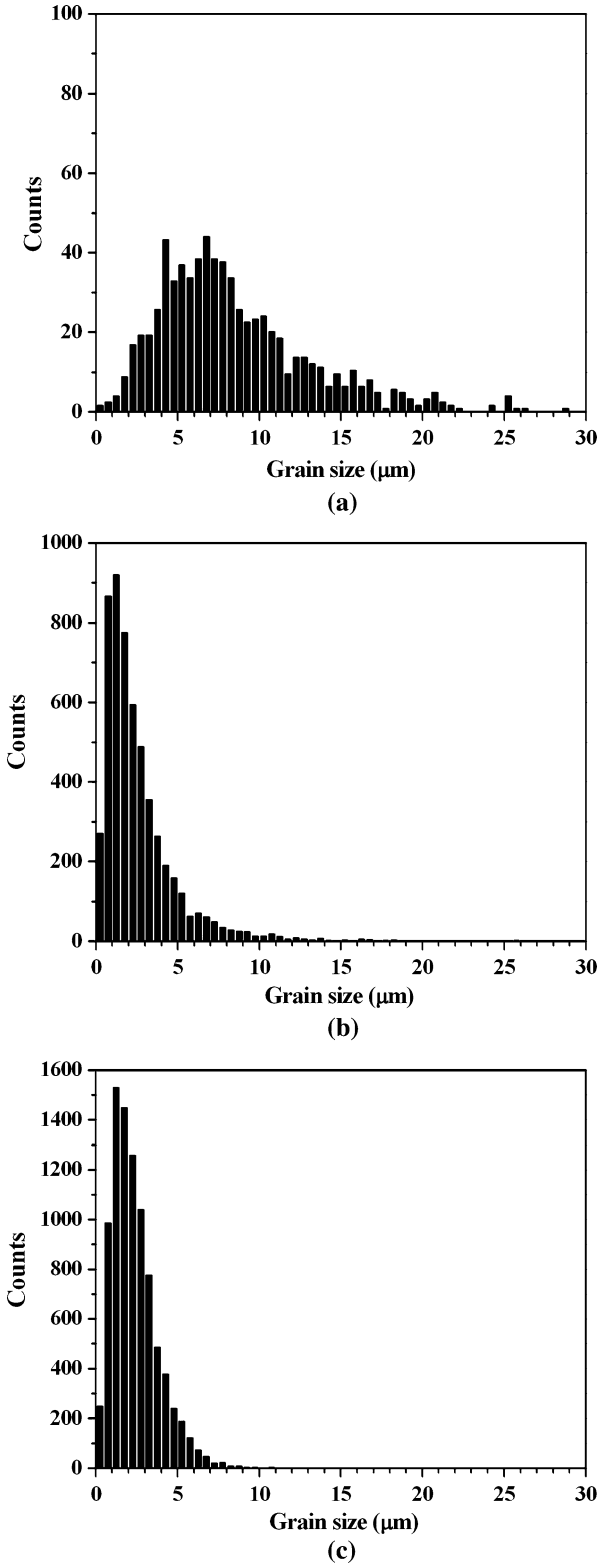

Fig. 5—Histograms showing grain size distribution (*a*) with no extrusion, (*b*) after 1 extrusion pass, and (*c*) after 4 extrusion passes. Route A was used, at 200 °C; extrusion speed was 10 cm/min.

B. *Process Route*

For this investigation, billets were extruded by the 120-deg die at 200 °C; the extrusion speed was 10 cm/min.

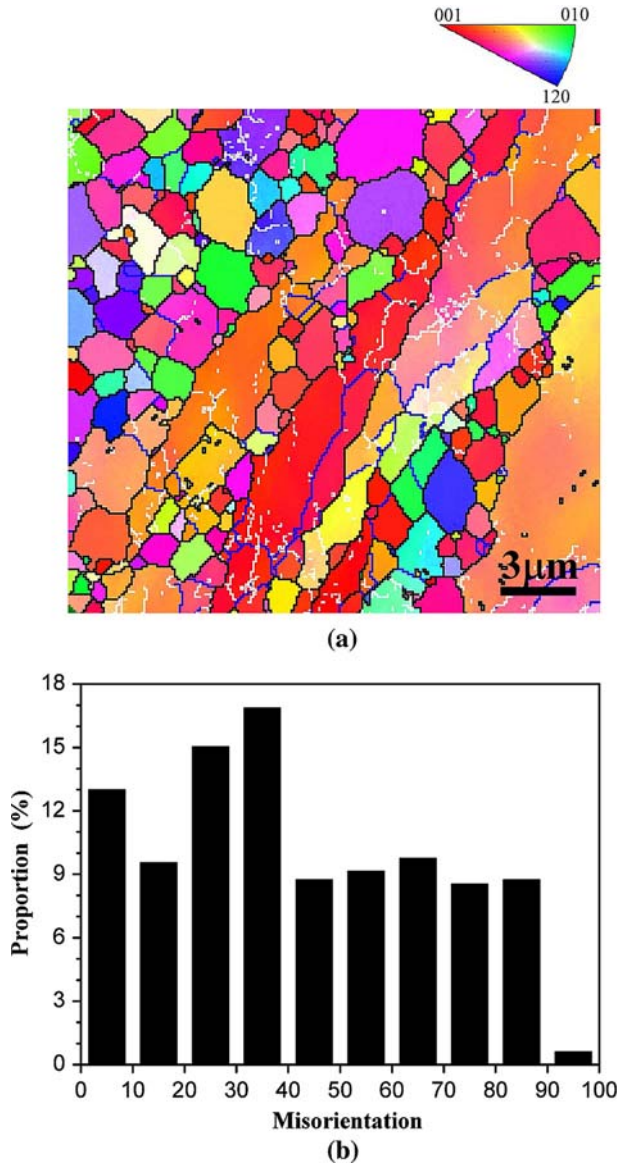

Fig. 6—(*a*) Orientation mapping from billet extruded at 200 °C for 1 pass. Black, blue, and white lines represent boundaries with misorientations larger than 15 deg, between 15 and 5 deg, and lower than 5 deg, respectively. (*b*) Histogram of boundary misorientations from billet extruded at 200 °C for 1 pass.

Three major process routes, namely, routes A, B_c, and C, were used. After 4 passes, both the shape and the size of the refined grains were virtually the same for all three routes. The evolution of grain size as a function of the number of extrusion passes for the three process routes was also found to be the same.

C. *Extrusion Speed (Strain Rate)*

Billets were extruded by the 120-deg die at 200 °C; two extrusion speeds, 10 and 0.8 cm/min, were tested. For all three routes, the same conclusion was obtained, that is, that a higher extrusion speed (strain rate) generates a smaller grain size (Figure 8). Due to the overlapping of the data points of the three routes, only the results from route B_c are presented in Figure 8.

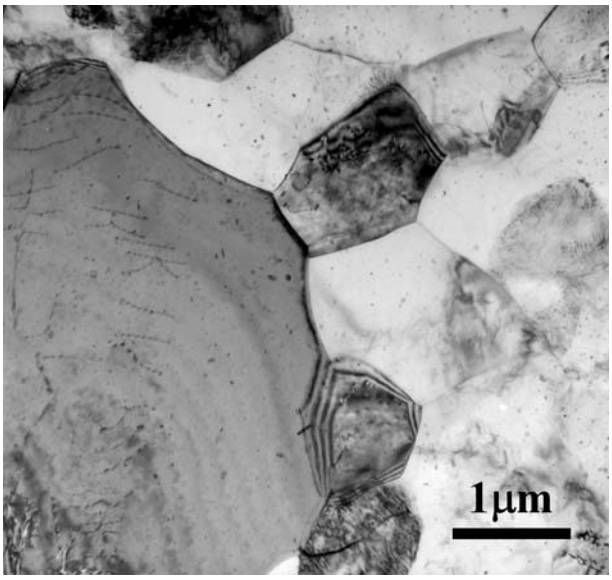

Fig. 7—TEM micrograph showing fine grains formed alongside a coarse grain after 1 extrusion pass at 200 °C. Note the grain-boundary fringes and the equilibrium configuration of fine grain boundaries.

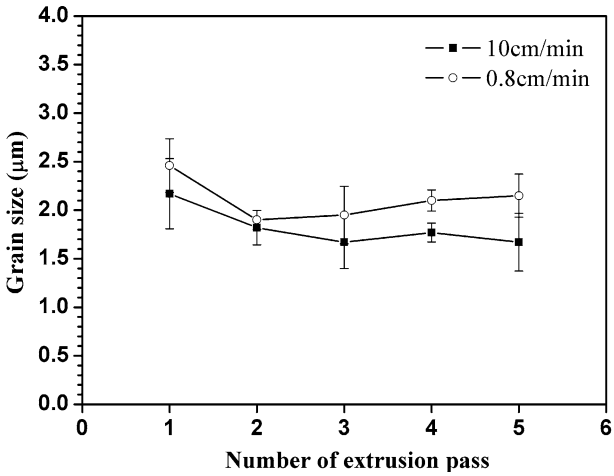

Fig. 8—Grain sizes obtained after extrusion at two different extrusion speeds. Higher extrusion speed generates smaller grain size. Extrusion at 200 °C using route B_c.

D. *Extrusion Temperature*

To investigate the effect of the extrusion temperature, billets were extruded by the 120-deg die using routes A and B_c; the extrusion speed was 10 cm/min. The evolution of the grain size in the billets extruded at three temperatures, 225 °C, 200 °C, and 175 °C, is shown in Figure 9. Figure 9 clearly shows that the lower the extrusion temperature used, the finer the grain size obtained. An extrusion temperature lower than 175 °C had been tried, but a billet without cracks was not obtained. When the extrusion speed was reduced to 3 cm/min, the extrusion could be successfully performed at 150 °C.

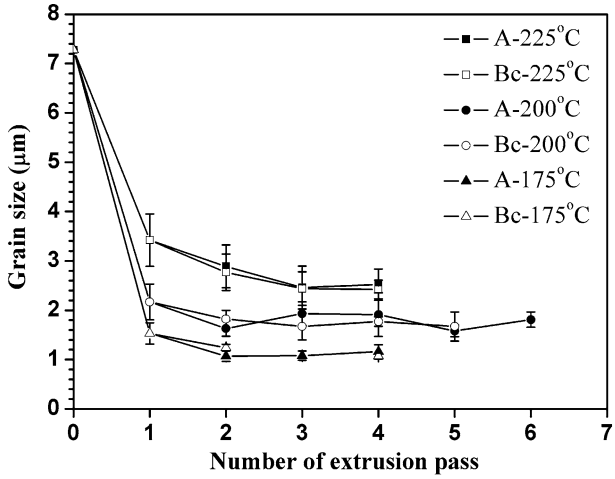

Fig. 9—Grain size obtained after extrusion at three different temperatures by three different routes. Higher extrusion temperature always generates larger grain size, irrespective of process route used.

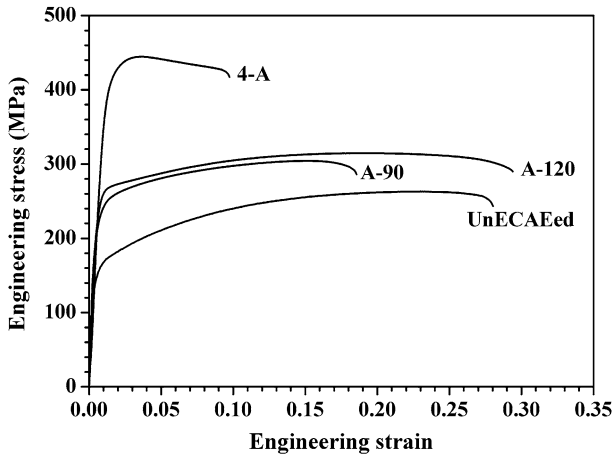

Fig. 10—Engineering stress-strain curves obtained from: (*a*) A-120: billet processed by Φ = 120-deg die; (*b*) A-90: billet processed by Φ = 90-deg die; (*c*) 4-A: billet processed by multitemperature extrusion procedure. (a) and (b) were extruded at 200 °C for 4 passes using route A; extrusion speed was 10 cm/min.

E. *Die Angle*

Billets were extruded at 200 °C using route A for 4 extrusion passes; the extrusion speed was 10 cm/min. The grain-refinement efficiencies produced by 90- and 120-deg dies were compared. Figure 3 demonstrates that, by using a 90-deg die angle, the grain size can be refined more quickly and to a finer degree than can be achieved by a 120-deg die angle. Despite the fact that the grain size obtained by using a 90-deg die angle was smaller, tensile tests showed that both the strength and the ductility produced by the 90-deg die angle were lower than those obtained by using a 120-deg die angle (Figure 10).

F. *Initial Grain Size*

Billets with different initial grain sizes were extruded by the 120-deg die using route A. Billets with a larger

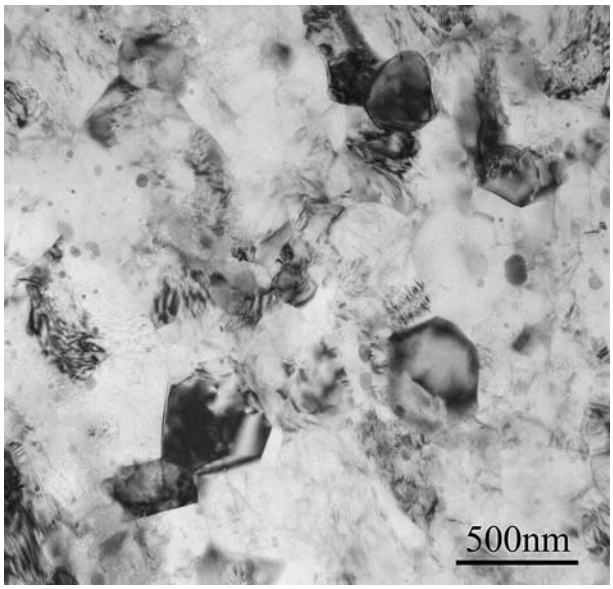

Fig. 11—Transmission electron micrograph showing the ultrafine-grained structure after multitemperature extrusion procedure. Average grain size of 0.37 μm was obtained.

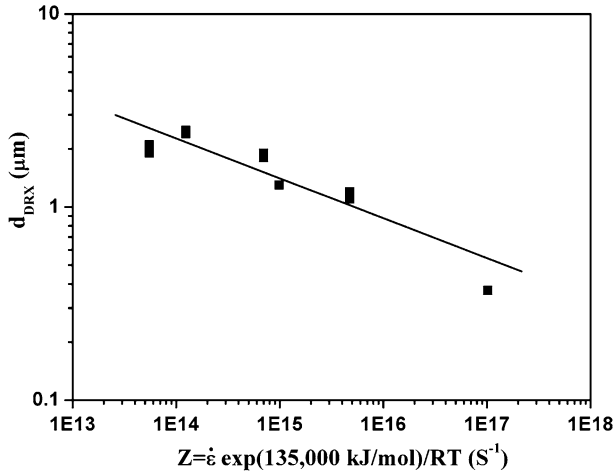

Fig. 12—Relationship between grain size of AZ31 Mg alloy subjected to ECAE and Zener–Hollomon parameter used.

initial grain size of 15 μm were obtained by annealing the billets at 400 °C for 24 hours. Under the same extrusion speed, the minimum workable extrusion temperature is lower for the billets with smaller grain sizes. For example, with an extrusion speed of 10 cm/min, a billet with a grain size of 7 μm could be extruded at 175 °C; the same was not true for the billet with a grain size of 15 μm.

G. *Multitemperature Extrusion*

An attempt was made to develop an extrusion procedure that can produce the finest possible grain size. Because a billet with a finer initial grain size could be extruded at a lower extrusion temperature, and because a lower extrusion temperature results in a finer grain size, a multitemperature extrusion procedure was accordingly developed that consists of four sequential steps: (1) 200 °C for 4 passes with a 10-cm/min extrusion speed, (2) 150 °C for 4 passes with a 3-cm/min extrusion speed, (3) 125 °C for 2 passes with a 1-cm/min extrusion speed, and (4) 115 °C for 2 passes with a 1-cm/min extrusion speed. In total, 12 extrusion passes were used. Route A was used for each temperature step; the billet was rotated 180 deg about the extrusion axis between steps (1), (2), and (3) and was rotated 90 deg between steps (3) and (4). The principles for developing this procedure will be given in Section IV. Because the grain size of the processed billets was too fine to be revealed by etching, TEM was used to measure the grain size of the billet. By measuring over 300 grains, the averaged grain size of this multistep-processed billet was found to be 0.37 μm, as shown in Figure 11. In Figure 11, several grains show diffraction contrast; the other grains cannot be seen under this diffraction condition. The ultrafine-grained AZ31 alloy has a record-high 0.2 pct proof strength of 372 MPa and a tensile strength of 445 MPa.[32] It also has reasonably good tensile ductility of 9.7 pct (Figure 10).

H. *Grain Size and the Zener–Hollomon Parameter*

As mentioned in Sections C and D, the grain size of the AZ31 Mg alloy subjected to ECAE depends on the extrusion speed and temperature. These two processing parameters can be used to calculate the Zener–Hollomon parameter: $Z = \dot{\varepsilon} \exp(Q/RT)$, where $\dot{\varepsilon}$ is the strain rate, Q the activation energy for the process, R the gas constant, and T the deformation temperature. For the dynamically recrystallized AZ31 Mg alloy, it was suggested that Q = 135 kJ/mole;[33] the strain rates were calculated according to Segal.[34] When the Zener–Hollomon parameters are plotted against the grain sizes (d), the relationship $d = AZ^{-n}$ can be established, where A and n are the fitting parameters (Figure 12). In dynamically recrystallized metals (including Mg alloys), the relationship $d = AZ^{-n}$ has been reported by several authors, *e.g.*, in References 33, 35, and 36.

IV. DISCUSSION

The present results show that the grain-refinement process of the AZ31 Mg alloy is distinctly different from that of fcc metals in several microstructural aspects.

For the AZ31 Mg alloy, the following is found.

(a) The fine grains are heterogeneously generated mainly from grain boundaries, as shown in Figures 2(b) and 3.
(b) The fine grains with high-angle grain boundaries are generated immediately after the first extrusion pass. With further extrusion, the number of fine grains increases, but the size of these fine grains is not refined further by additional extrusion passes, as shown in Figures 2 and 5 through 7.
(c) The fine grains are generated in an equiaxed shape, as shown in Figures 2 and 3.

For fcc metals, the following is found.

(a) The fine grains are homogeneously formed; this is because, for fcc metals, fine grains are formed by the gradual transformation of dislocation cell walls into grain boundaries.[1–4]
(b) Dislocation cells with low-angle dislocation walls are formed after the first few extrusion passes. Fine grains with high-angle grain boundaries are formed only after many extrusion passes. The size of these cells is gradually refined by the extrusion passes; meanwhile, dislocation walls are transformed into grain boundaries.[1,4]
(c) Fine grains with an equiaxed shape are transformed from dislocation cells that have a "checkerboard pattern."[1,4]

The discovery of the serration of the original grain boundaries and the nucleation of the fine grains at the original grain boundaries (Figures 2(b) and 3) indicates that dynamic recrystallization occurred.[33,37–39] For dynamic recrystallization, new grains generally nucleate at the original grain boundaries; subsequently, more fine grains nucleate at the boundaries of the newly formed fine grains. In this way, recrystallized fine grains are formed and broaden as dynamic recrystallization proceeds; eventually, recrystallized fine grains replace the original coarse grains.[37] One important characteristic of dynamic recrystallization is that the recrystallized grains remain virtually unchanged as deformation proceeds.[33,37] Once the grain-refinement process of the AZ31 Mg alloy is understood as a dynamic recrystallization process, it can explain why (1) the heterogeneous distribution of fine grains was found during the first few extrusion passes, (2) the size of the fine grains was not gradually refined by more extrusion passes, (3) the newly formed fine grains are equiaxed and have high-angle grain boundaries, and (4) the relationship between the grain size and the Zener–Hollomon parameter, $d = AZ^{-n}$, was found. The grain-refinement process of Mg alloys by ECAE that is suggested in the literature, such as the gradual transformation of low-angle subgrain boundaries into high-angle grain boundaries by the absorption of dislocations during successive extrusion passes[23,29] or the growth of recovered subgrain boundaries due to dynamic annealing during extrusion,[28] cannot explain the microstructural characteristics found in the present research.

Because the grain-refinement process of the AZ31 Mg alloy is different from that of fcc metals, the effect of ECAE processing parameters on grain refinement is, therefore, different and will be discussed as follows.

(a) The number of extrusion passes (imposed plastic strain): Once dynamic recrystallization is completed, the material is in a steady state and further deformation of the material cannot change the grain size. This is the reason that the grain size of a billet in the present research remained unchanged after 4 extrusion passes (equivalent strain of 2.68). Jin *et al.*[29] reported the same finding for the Mg alloy. For fcc metals, *e.g.*, Al, which requires an equivalent strain of more than approximately 8 to produce fine grains with enough high-angle grain boundaries,[3,40] this is the reason that many authors[20,21,24–27,29] used a large number of extrusion passes, *e.g.*, 6 or 8 passes, to process their Mg alloys. It is expected that billets with a larger initial grain size will require a higher plastic strain to complete dynamic recrystallization, because larger grains provide less grain-boundary area for the nucleation of new fine grains. In general, the plastic strain needed to obtain a uniform fine-grained structure in an Mg alloy is less than that needed for fcc metals.
(b) Process route: As mentioned earlier, for fcc metals, route B_c has been found to be the most effective route in terms of grain refinement; therefore, most authors[16–29] used route B_c to process their Mg alloys. However, the present results indicate that process routes A, B_c, and C have the same grain-refinement effect. Although all three routes produce a similar grain size, route A is recommended for processing the AZ31 Mg alloy, because it generates the greatest strength among these three routes due to the texture effect.[32]
(c) Extrusion speed (strain rate): Figure 8 shows that a higher extrusion speed can generate smaller grains. This result is consistent with the behavior of dynamic crystallization, specifically, that a higher strain rate could generate smaller recrystallized grains.[33,35,36] For fcc metals, grain refinement is not achieved by dynamic recrystallization; therefore, Berbon *et al.*[15] found that the extrusion speed had no influence on the grain size of aluminum and its alloys subjected to ECAE. Using a high extrusion speed to process the AZ31 Mg alloy has one disadvantage: A high extrusion speed decreases the workability of the billet at low extrusion temperatures. As mentioned in Section III, by using an extrusion speed of 10 cm/min, the minimum workable extrusion temperature is 175 °C; when the extrusion speed decreased to 3 cm/min, the workable extrusion temperature dropped to below 150 °C. Therefore, at extrusion temperatures lower than 175 °C, the extrusion speed has to be reduced to less than 10 cm/min. The use of a low extrusion speed to improve the workability of titanium and 4340 steel[11] and the AZ31 alloy[41] has been reported previously.
(d) Extrusion temperature: Because the grain size of the AZ31 Mg alloy subjected to ECAE is determined by the dynamic recrystallization process and because it was reported in the literature that a lower deformation temperature generated smaller dynamically recrystallized grains,[33,35,36] it is therefore expected that a lower ECAE extrusion temperature gives a smaller grain size. Despite the fact that a low extrusion temperature is desirable for producing an ultrafine-grained Mg alloy, however, there is a minimum workable extrusion temperature for a certain extrusion speed. The lower the extrusion speed, the lower the minimum workable extrusion temperature. The minimum workable extrusion temperature also depends on the initial grain size of the billet: The smaller the

initial grain size, the lower the minimum workable extrusion temperature. For example, when using an extrusion speed of 10 cm/min, the minimum workable extrusion temperature of a billet with a grain size of 7 μm is 175 °C; for a billet with a grain size of 15 μm, however, the minimum workable extrusion temperature is higher than 175 °C. It should noted that it has been reported by Su *et al.*[28] that extrusion at a higher temperature gives a larger grain size. However, these authors thought that the larger grain size was due to the excessive grain growth caused by dynamic annealing at a higher extrusion temperature. In addition, the present authors believed that different extrusion temperatures generate different sizes of dynamic recrystallized grains, as discussed earlier.

(e) Die angle: Figure 3 shows that a smaller grain size can be obtained by using the die with the 90-deg die angle. The same result was found in aluminum.[8] Despite the production of a smaller grain size by using 90-deg die angle, it was found that, due to the texture effect,[42] the strength of the billet extruded by a 90-deg die angle was lower than the strength of the billet extruded by a 120-deg die angle. It was also found that, when using a 90-deg die angle, the billet was more susceptible to surface cracking.[42]

(f) Initial grain size: The initial grain size has never been reported to have any effect on the grain refinement of fcc metals. In contrast, the current research found that the initial grain size had a great effect on the grain refinement of the AZ31 Mg alloy. The larger the initial grain size, the higher the extrusion temperature needed; the higher the extrusion temperature, the larger the final grain size produced. The high extrusion temperature needed for a large-grained billet is related to the low workability of the billet. For large-grained Mg alloys, the deformation limited by basal slip causes poor grain-boundary compatibility. However, a higher portion of nonbasal slip can be activated in small-grained Mg alloys; this gives better compatibility between the grains[43,44] and results in better workability. Increasing the extrusion temperature can also increase the activity of the nonbasal slip[45] and can, therefore, improve the workability of Mg alloys.

The Mg alloys extruded at successive decreasing temperatures for each extrusion pass have been reported;[23,46] however, these authors provided no reason for their extrusion procedure. For the present research, the development of the multitemperature extrusion procedure is accomplished according to the guidelines obtained from the present results, as discussed earlier. Route A and a 120-deg die angle are chosen, because they give higher strength. A single-temperature extrusion cannot be used to obtain an ultrafine-grained AZ31 Mg alloy, because to obtain such a fine grain size, the extrusion temperature has to be very low; the AZ31 Mg alloy with a conventional grain size, however, cannot be extruded at such a low temperature. The way to improve the workability of a billet at low temperatures is to reduce the grain size of the billet. The multitemperature extrusion procedure is therefore developed, because extrusion at a workable temperature could refine the grain size for the next lower extrusion temperature, which is not a workable temperature for the larger initial grain size. A different extrusion speed is used at a different extrusion temperature, in order to have the required workability at different extrusion temperatures. Lower extrusion temperatures have poorer workability; therefore, the extrusion speed needs to be reduced.

When a billet was extruded using the multitemperature extrusion procedure without rotation about the extrusion axis between different temperature steps, cracks formed and the extrusion failed. The cracks were always found on the upper surface of the billet. In line with Figueiredo *et al.*,[47] it was decided to rotate the billet 180 deg about the extrusion axis between each temperature step. Figueiredo *et al.* used finite element simulation and found that the material damage factor is highest at the upper surface of a billet, when the strain-rate sensitivity of the material is not zero. If a billet is rotated 180 deg after several extrusion passes, it can limit the accumulation of damage on the upper surface of the billet that results from the large number of extrusion passes. Another advantage of the 180-deg rotation of a billet is that it may prevent the growth of any fine cracks, if formed, during each temperature step, because by the 180-deg rotation of a billet, the flow direction of the material is reversed.[48,49] When the 180-deg rotation between each temperature step was performed, a billet could be successfully extruded down to 125 °C, but not to 115 °C. It was thought that perhaps the upper surface of the billet had already accumulated a certain amount of surface damage during the extrusion at 150 °C (step 2); once the surface was turned to the upper surface position again at 115 °C (step 4), it could not withstand any more damage and failure occurred. It was, therefore, decided to rotate the billet 90, instead of 180, deg after extrusion at 125 °C (step 3), to avoid having the upper surface of the billet at the 150 °C extrusion step become the upper surface again at 115 °C. In this way, the multitemperature extrusion procedure was successfully completed. Due to the very effective grain refinement of this procedure, the processed billet has the record high strength of the AZ31 alloy with reasonably good ductility.[32] The success of the development of this ECAE procedure proves that ECAE can offer a good opportunity for the development of high-strength Mg alloys.

It is interesting to know whether the present results can be applied to other hcp metals, *e.g.*, Ti. In the literature, there are several reports on the microstructure of Ti subjected to ECAE, *e.g.*, References 50 through 53; however, no occurrence of dynamic recrystallization was reported in Ti subjected to ECAE. The extrusion temperatures used in these articles were between 0.24 and 0.45 T_m, where T_m is the melting point of Ti. Because the effects of the processing parameters on the grain refinement of the AZ31 Mg alloy found in the present research are due to the occurrence of dynamic

recrystallization during ECAE, it is certain that if dynamic recrystallization does not occur during ECAE, the conclusions drawn from the present research cannot be applied. The extrusion temperatures used in the present research are between 0.46 and 0.59 T_m. Here, the solidus temperature of the AZ31 alloy, 566 °C, is adopted as its melting point.

V. CONCLUSIONS

The present results show that the grain-refinement process of the AZ31 Mg alloy fabricated by ECAE is dynamic recrystallization, which is different from that of fcc metals. Because of the difference, the effects of the processing parameters on the grain refinement of the AZ31 Mg alloy are quite different from those for fcc metals.

During extrusion, once dynamic recrystallization is completed, excessive extrusion passes provide no effect on grain refinement. The plastic strain required for obtaining a uniform fine-grained structure in the AZ31 Mg alloy is much less than that required for fcc metals. All process routes give the same grain-refinement effect. Route A gives the highest strength among all routes; this can be attributed to the texture effect. A low extrusion temperature is desirable for producing a fine-grained AZ31 Mg alloy; however, for a certain extrusion speed, there is a minimum workable extrusion temperature. The lower the extrusion speed, the lower the minimum workable extrusion temperature. The minimum workable extrusion temperature also depends on the initial grain size of a billet; the smaller the initial grain size, the lower the minimum workable extrusion temperature.

A multitemperature extrusion procedure has been developed that can produce a submicron-grained AZ31 Mg alloy having a grain size as small as 0.37 μm. This submicron-grained AZ31 Mg alloy has a record high strength accompanied by reasonably good tensile ductility. The success of the development of this ECAE procedure proves that ECAE can offer a good opportunity for producing high-strength Mg alloys by grain refinement.

ACKNOWLEDGMENT

The authors thank the National Science Council of Taiwan for the support of their research through Contract Nos. NSC 93-2216-E110-007 and NSC 94-2216-E110-003.

REFERENCES

1. Y. Iwahashi, Z. Horita, M. Nemoto, and T.G. Langdon: *Acta Mater.*, 1997, vol. 45, pp. 4733–41.
2. A. Gholinia, P.B. Prangnell, and M.V. Markushev: *Acta Mater.*, 2000, vol. 48, pp. 1115–30.
3. P.L. Sun, P.W. Kao, and C.P. Chang: *Scripta Mater.*, 2004, vol. 51, pp. 565–70.
4. C.P. Chang, P.L. Sun, and P.W. Kao: *Acta Mater.*, 2000, vol. 48, pp. 3377–85.
5. S.R. Agnew and J.R. Weertman: *Mater. Sci. Eng., A*, 1998, vol. 244, pp. 145–53.
6. M.H. Shih, C.Y. Yu, P.W. Kao, and C.P. Chang: *Scripta Mater.*, 2001, vol. 45, pp. 793–99.
7. F. Dalla Torre, R. Lapovok, J. Sandlin, P.F. Thomson, C.H.J. Davies, and E.V. Pereloma: *Acta Mater.*, 2004, vol. 52, pp. 4819–32.
8. K. Nakashima, Z. Horita, M. Nemoto, and T.G. Langdon: *Acta Mater.*, 1998, vol. 46, pp. 1589–99.
9. P.L. Sun, P.W. Kao, and C.P. Chang: *Metall. Mater. Trans. A*, 2004, vol. 35A, pp. 1359–68.
10. Y. Iwahashi, Z. Horita, M. Nemoto, and T.G. Langdon: *Acta Mater.*, 1998, vol. 46, pp. 3317–31.
11. S.L. Semiatin, V.M. Segal, R.E. Goforth, N.D. Frey, and D.P. DeLo: *Metall. Mater. Trans. A*, 1999, vol. 30A, pp. 1425–35.
12. A. Yamashita, D. Yamaguchi, Z. Horita, and T.G. Langdon: *Mater. Sci. Eng., A*, 2000, vol. 287, pp. 100–06.
13. Y.C. Chen, Y.Y. Huang, C.P. Chang, and P.W. Kao: *Acta Mater.*, 2003, vol. 51, pp. 2005–15.
14. Y.Y. Wang, P.L. Sun, P.W. Kao, and C.P. Chang: *Scripta Mater.*, 2004, vol. 50, pp. 613–17.
15. P.B. Berbon, M. Furukawa, Z. Horita, M. Nemoto, and T.G. Langdon: *Metall. Mater. Trans. A*, 1999, vol. 30A, pp. 1989–97.
16. K. Matsubara, Y. Miyahara, Z. Horita, and T.G. Langdon: *Acta Mater.*, 2003, vol. 51, pp. 3073–84.
17. K. Matsubara, Y. Miyahara, Z. Horita, and T.G. Langdon: *Metall. Mater. Trans. A*, 2004, vol. 35A, pp. 1735–44.
18. Y. Miyahara, K. Matsubara, Z. Horita, and T.G. Langdon: *Metall. Mater. Trans. A*, 2005, vol. 36A, pp. 1705–11.
19. L. Cisar, Y. Yoshida, S. Kamado, Y. Kojima, and F. Watanabe: *Mater. Trans.*, 2003, vol. 44, pp. 476–83.
20. T. Mukai, M. Yamanoi, H. Watanabe, and K. Higashi: *Scripta Mater.*, 2001, vol. 45, pp. 89–94.
21. Y. Yoshida, L. Cisar, S. Kamado, and Y. Kojima: *Mater. Trans.*, 2003, vol. 44, pp. 468–75.
22. S.Y. Chang, S.W. Lee, K.M. Kang, S. Kamado, and Y. Kojima: *Mater. Trans.*, 2004, vol. 45, pp. 488–92.
23. H.K. Kim and W.J. Kim: *Mater. Sci. Eng., A*, 2004, vol. 385, pp. 300–08.
24. S.R. Agnew, J.A. Horton, T.M. Lillo, and D.W. Brown: *Scripta Mater.*, 2004, vol. 50, pp. 377–81.
25. W.J. Kim and H.T. Jeong: *Mater. Trans.*, 2005, vol. 46, pp. 251–58.
26. K. Xia, J.T. Wang, X. Wu, G. Chen, and M. Gurvan: *Mater. Sci. Eng., A*, 2005, vols. 410–411, pp. 324–27.
27. H.K. Lin, J.C. Huang, and T.G. Langdon: *Mater. Sci. Eng., A*, 2005, vol. 402, pp. 250–57.
28. C.W. Su, L. Lu, and M.O. Lai: *Mater. Sci. Eng., A*, 2006, vol. 434, pp. 227–36.
29. L. Jin, D. Lin, D. Mao, X. Zeng, B. Chen, and W. Ding: *Mater. Sci. Eng., A*, 2006, vol. 423, pp. 247–52.
30. M. Eddahbi, J.A. del Valle, M.T. Perez-Prado, and O.A. Ruano: *Mater. Sci. Eng., A*, 2005, vols. 410–411, pp. 308–11.
31. M. Furukawa, Y. Iwahashi, Z. Horita, M. Nemoto, and T.G. Langdon: *Mater. Sci. Eng., A*, 1998, vol. 257, pp. 328–32.
32. S.X. Ding, W.T. Lee, C.P. Chang, L.W. Chang, and P.W. Kao: *Scripta Mater.*, 2008, vol. 59, pp. 1006–09.
33. A.G. Beer and M.R. Barnett: *Metall. Mater. Trans. A*, 2007, vol. 38A, pp. 1856–67.
34. V.M. Segal: *Mater. Sci. Eng., A*, 2004, vol. 386, pp. 269–76.
35. S. Wierzbinski, A. Korbel, and J.J. Jonas: *Mater. Sci. Technol.*, 1992, vol. 8, pp. 153–58.
36. S.M. Fatemi-Varzaneh, A. Zarei-Hanzaki, and H. Beladi: *Mater. Sci. Eng., A*, 2007, vol. 456, pp. 52–57.
37. F.J. Humphreys and M. Hatherly: *Recrystallization and Related Annealing Phenomena*, Pergamon, Oxford, United Kingdom, 1996, pp. 373–74.
38. S.E. Ion, F.J. Humphreys, and S.H. White: *Acta Metall.*, 1982, vol. 30, pp. 1909–19.
39. T. Al-Samman and G. Gottstein: *Mater. Sci. Eng., A*, 2008, vol. 490, pp. 411–20.
40. S.D. Terhune, D.L. Swisher, K. Oh-ishi, Z. Horita, T.G. Langdon, and T.R. McNelley: *Metall. Mater. Trans. A*, 2002, vol. 33A, pp. 2173–84.

41. F. Kang, J.T. Wang, and Y. Peng: *Mater. Sci. Eng., A*, 2008, vol. 487, pp. 68–73.
42. S.X. Ding: Doctoral Thesis, National Sun Yat-sen University, Taiwan, 2008.
43. J. Koike: *Mater. Sci. Forum*, 2004, vols. 449–452, pp. 665–68.
44. J. Koike: *Metall. Mater. Trans. A*, 2005, vol. 36A, pp. 1689–96.
45. H. Miura, X. Yang, T. Sakai, H. Nogawa, S. Miura, Y. Watanabe, and J.J. Jonas: *Philos. Mag.*, 2005, vol. 85, pp. 3553–65.
46. A. Mussi, J.J. Blandin, L. Salvo, and E.F. Rauch: *Acta Mater.*, 2006, vol. 54, pp. 3801–09.
47. R.B. Figueiredo, P.R. Cetlin, and T.G. Langdon: *Acta Mater.*, 2007, vol. 55, pp. 4769–79.
48. M. Furukawa, Z. Horita, and T.G. Langdon: *Mater. Sci. Eng., A*, 2002, vol. 332, pp. 97–109.
49. J.R. Bowen, A. Gholinia, S.M. Roberts, and P.B. Prangnell: *Mater. Sci. Eng., A*, 2000, vol. 278, pp. 87–99.
50. D.H. Shin, I. Kim, J. Kim, and Y.T. Zhu: *Mater. Sci. Eng., A*, 2002, vol. 334, pp. 239–45.
51. D.H. Shin, I. Kim, J. Kim, Y.S. Kim, and S.L. Semiatin: *Acta Mater.*, 2003, vol. 51, pp. 983–96.
52. V.V. Stolyarov, Y.T. Zhu, I.V. Alexandrov, T.C. Lowe, and R.Z. Valiev: *Mater. Sci. Eng., A*, 2003, vol. 343, pp. 43–50.
53. I. Kim, J. Kim, D.H. Shin, C.S. Lee, and S.K. Hwang: *Mater. Sci. Eng., A*, 2003, vol. 342, pp. 302–10.